Journal Name

ARTICLE

A Na^+ conducting hydrogel for protection of organic electrochemical transistors

Received 00th January 20xx,
Accepted 00th January 20xx

DOI: 10.1039/x0xx00000x

www.rsc.org/

I. del Agua,[a, b] L. Porcarelli,[a] V. F. Curto,[b,c] A. Sanchez-Sanchez,[b, c] E. Ismailova,[b] G. G. Malliaras,[b,c] and D. Mecerreyes*[a, d]

Organic electrochemical transistors (OECTs) are being intesively developed for applications in electronics and biological interfacing. These devices rely on ions injected in a polymer film from an aqueous liquid electrolyte for their operation. However, the development of solid or semi-solid electrolytes are needed for future integration of OECTs into flexible, printed or conformable bioelectronic devices. Here, we present a new polyethylene glycol hydrogel with high Na^+ conductivity which is particularly suitable for OECTs. This novel hydrogel was synthesized using cost-effective photopolymerization of poly(ethylene glycol)-dimethacrylate and sodium acrylate. Due to the high water content (83% w/w) and the presence of free Na^+, the hydrogel showed high ionic conductivity values at room temperature (10^{-2} S cm^{-1}) as characterized by electrochemical impedance spectroscopy. OECTs made using this hydrogel as a source of ions showed performance that was equivalent to that of OECTs employing a liquid electrolyte. They also showed improved stablity, with only a 3% drop in current after 6 h of operation. This hydrogel paves the way for the replacement of liquid electrolytes in high performance OECTs bringing about advantages in terms of device integration and protection.

Introduction

Organic electrochemical transistors (OECTs) are attracting a great deal of interest for applications including electrophysiology,[1–3] medical diagnostics,[4,5] large-area electronics[6] and neuromorphic computing.[7] These devices leverage the ability of polymers such as poly(3,4-ethylenedioxythiophene) doped with polystyrene sulfonate (PEDOT:PSS) to transport both electronic and ionic charges. In a typical OECT configuration, the channel connecting the source and the drain electrodes is made of a PEDOT:PSS film. The PEDOT channel is also in contact with an electrolyte in which a gate electrode is immersed. Under these conditions, large drain current can flow in the highly doped PEDOT channel. However, applying a positive potential to the gate electrode causes cations to be injected from the electrolyte into the PEDOT:PSS film. This decreases the amount of doping of PEDOT, hence the drain current.[8,95,10] This coupling between ionic and electronic charges in OECTs leads to a large modulation in the drain current by a small gate voltage, and makes these devices efficient amplifiers of biological signals.[11,12] It also allows OECTs to be fabricated in planar architectures where the gate electrode is placed on the same substrate as the channel, which is desirable for large area electronics but difficult to achieve with silicon transistors.[12,13]

While considerable attention has been paid to the development of conjugated polymers that make up the channel of OECTs, relatively little effort has been devoted to the electrolyte that acts as the source of ions in these devices. The vast majority of high performance OECTs reported thus far employ aqueous liquid electrolytes which limits their applicability. However, the development of solid or semi-solid polymer electrolytes are needed for future integration of OECTs into protected, flexible, printed or conformable bioelectronic devices.[14,15] The development of gel electrolytes is of particular interest, as these materials combine soft mechanical properties, which are of interest for flexible devices and biological interfacing,[16] while avoiding the processing and leaking issues associated with the use of liquids into the device.[17–20] The ionic conductivity of the gel determines the polarization response time of the channel thus having a major importance.[20] However, since solid electrolytes present lower ionic conductivity values than the liquid electrolytes, this results in low switching response devices.[19]

In this work, a novel hydrogel with high ionic conductivity for application in OECTs is presented. The hydrogel was synthesized by cost-effective in-situ photo-polymerization of acrylate-PEG monomers in rapid way and with high degree of control over the final hydrogel structure and shape. PEG was selected as it yields hydrogels that show high water content retention[21] and are biocompatible.[22] Sodium was selected as the only mobile ion of the hydrogel due to its small size which favors the ion mobility and the interaction with the conducting

[a] POLYMAT University of the Basque Country UPV/EHU, Joxe Mari Korta Center, Avda. Tolosa 72, 20018 Donostia-san Sebastian, Spain.
[b] Department of Bioelectronics, Ecole Nationale Supérieure des Mines, CMP-EMSE, MOC, 13541 Gardanne, France.
[c] Current address: Electrical Engineering Division, Department of Engineering, University of Cambridge, 9 JJ Thomson Avenue, Cambridge, CB3 0FA, United Kingdom
[d] Ikerbasque, Basque Foundation for Science, E-48011 Bilbao, Spain.
Electronic Supplementary Information (ESI) available: [details of any supplementary information available should be included here]. See DOI: 10.1039/x0xx00000x

polymer PEDOT:PSS. Our sodium conducting hydrogel was formed by copolymerization of sodium acrylate ionic monomer with neutral monomers containing PEG. The hydrogel was characterized in terms of mechanical stability and ionic conductivity. More importantly, we report how it facilitates the electrochemical response of PEDOT:PSS and its high performance in OECTs.

Results and discussion

Na^+ conducting hydrogels synthesis and characterization

Poly(ethylene glycol) (PEG) crosslinked hydrogels containing mobile sodium ions were synthesized by photo-polymerization according to the reaction shown in Scheme 1. In a typical reaction, poly(ethylene glycol) acrylate (PEGA) and sodium acrylate (NaA) were UV copolymerized in the presence of a given amount of water and poly(ethylene glycol) diacrylate (PEGDA). PEGA (11 % w/w) was used to enhance water retention of the hydrogel, while PEGDA was chosen to obtain a water insoluble network, as it contains two reactive groups capable of cross-linking the hydrogel acrylate backbone. A low amount of PEGDA was used (2 % w/w) in order to ensure mechanical stability without stiffening the hydrogel. Sodium acrylate was present in 4 % w/w, providing mobile sodium cations, while the negative charges were bonded onto the polymeric backbone forming an anionic polyelectrolyte network.

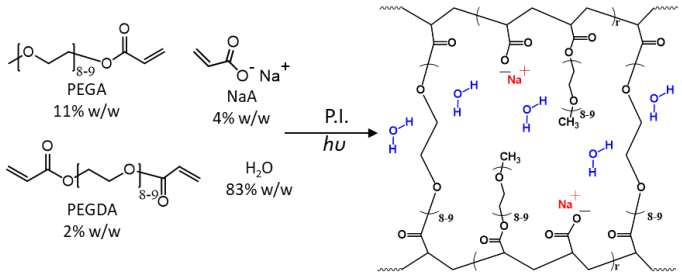

Scheme 1 Synthesis of Na^+ conducting hydrogels. Photopolymerization reaction of PEGA, PEGDA, and NaA in the presence of water.

Fig. S1 shows the FTIR-ATR spectra of hydrogels having 83 and 3% w/w water content. The characteristic bands of water dominated the spectrum of the 83% w/w hydrogel. The spectrum of the 3% w/w hydrogel contained the distinctive stretch of the ester carbonyl group C=O at 1729 cm^{-1} and the distinctive CO ether stretches at 1096 cm^{-1}. Other bands corresponding to the CH stretches at 2866 cm^{-1}, CH_2 bending stretches at 1450 cm^{-1}, and CH_3 bending stretches at 1350 cm^{-1} were also observed. A broad band at 3450 cm^{-1} was observed due to water contained into the sample. Finally, quantitative monomer conversion was demonstrated by the absence of the characteristic C=C stretch bands in the fingerprint region at 1640 and 660 cm^{-1}. ^{1}H-NMR measurement also proved the absence of un-reacted monomer in the hydrogels (Fig S2). Environmental SEM pictures of an 83% w/w hydrogel are shown in Fig. S3. The morphological characterization of the hydrogel revealed a homogeneous smooth surface without relevant features.

The ionic conductivity of the hydrogel changed with the composition of the hydrogel, as shown in Fig. 1a where the ionic conductivities of the hydrogels synthetized with different water contents are plotted. The highest ionic conductivity measured at room temperature was 3.6 10^{-2} S cm^{-1}, for the hydrogel containing 83% w/w of water. When the water content of the hydrogel was lowered to 63 % w/w, the conductivity was reduced to 1.1 10^{-2} S cm^{-1}. Further reducing water content to 43 % w/w lead to a drop in the conductivity to 1.6 10^{-3} S cm^{-1}. The lowest conductivity measured at room temperature was 6.9 10^{-5} S cm^{-1} in the hydrogel containing only 3 % w/w water. As expected, the highest conductivity was achieved when the water content was the highest since the water helps the ionic mobility. The hydrogel with 83% w/w water content presents high conductivity when compared to other PEG-based hydrogels present in literature[23] and for this reason, it was selected for further study and device integration as it showed the highest ionic conductivity.

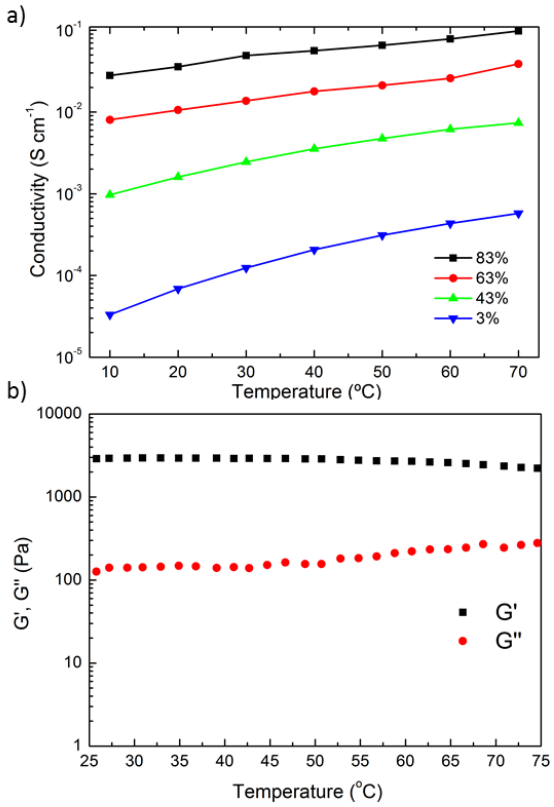

Figure 1 Na^+ conducting hydrogel characterization. Ionic conductivity of hydrogels at different water contents at 83, 63, 43, and 3% w/w (a), Rheological behavior, G' and G" evolution with temperature for hydrogel 83% w/w (b).

Rheological properties of the 83% w/w hydrogel were analyzed by frequency sweep measurements. We investigated the evolution of elastic (G') and viscous (G'') moduli of the hydrogel as a function of the frequency (Fig. S4) and temperature (Fig. 1b). G' modulus was higher than G'' on the whole frequency range and independent of frequency, which is typical of a solid-like behaviour. Interestingly, the hydrogel

showed high temperature stability in the temperature range from 25 to 75 °C.

The major motivation behind this work was to synthesize a hydrogel capable to enhance the electrochemical response of PEDOT:PSS. For this reason, our hydrogel was employed as an electrolyte in a simple test to investigate its ability to reversibly dope PEDOT:PSS films with the mobile sodium cation (Fig. 2). Usually, the speed of the process depends on the hydrated radius of the ions (the smaller the faster)[24] in the electrolyte media, and the swelling of the PEDOT:PSS film when in contact with the electrolyte. Therefore, a hydrogel with high water content and containing mobile Na^+ should be an appropriate gel electrolyte for modulating PEDOT:PSS doping. We evaluated the ability of the hydrogel to manipulate the doping of PEDOT:PSS films by applying a potential in between the two contacts (+1V, -1V). The results were already

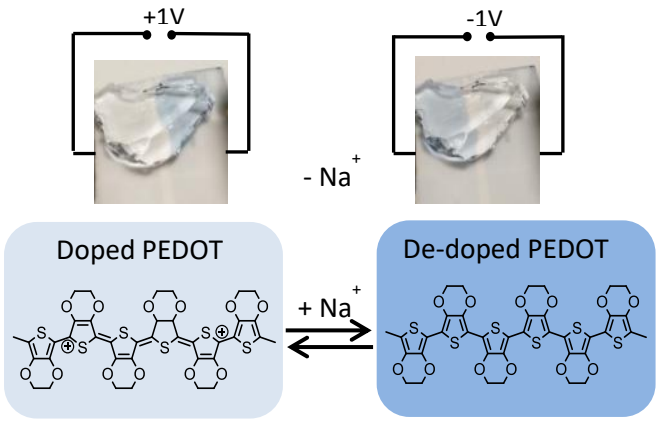

Figure 2. PEDOT switching test. Two spin-coated PEDOT:PSS electrodes on a glass slide connected by the hydrogel.

visible to the naked eye since the electrochromic properties of PEDOT. When a potential difference was applied across the two electrodes (Fig. 2), Na^+ ions penetrated the negatively-biased PEDOT:PSS electrode. The insertion of sodium induced PEDOT de-doping and the polymer film turned dark blue. Upon extraction of sodium ions from the film at the reversed potential, PEDOT chains were doped and polymer films turned light blue.

This simple test was fully reversible, as we were able to perform more than 100 cycles. In fact, this experiment indicated that our hydrogel was able to provide cations to the doping process without degradation of the film.[9,25] This initial characterization study showed good interaction between PEDOT:PSS and our hydrogel and prompted the evaluation of this material in OECTs.

Na^+ conducting hydrogel as electrolyte for OECTs

In the previous section we showed how the Na^+ hydrogel can be used for the selective doping and de-doping of PEDOT:PSS. Following these promising results, we studied the performance of the hydrogel electrolyte when coupled together with an OECT in which PEDOT:PSS was used as the active layer of the transistor channel. The vast majority of the OECTs reported in literature operate in liquid aqueous electrolyte. In this configuration a positive potential applied to the gate electrode (typically Ag/AgCl) causes the injection of cations in the PEDOT:PSS film followed by a decrease in the drain current. As a mean of easy integration of the hydrogel electrolyte with the OECT, we employed a planar transistor in which a PEDOT:PSS gate electrode was used to bias the device. The solution was casted on top of the OECT (both transistor channel and gate electrode) and UV photopolymerization was carried out to form the hydrogel. The OECT schematic drawing in Fig. 3a shows the cross-section of the device architecture and the wiring scheme used to operate the device. It should be noted here that future integration of the Na^+ hydrogel with OECTs could also be performed using photolithographic tools to finely control/tune the device and hydrogel geometry.

To characterize the performance of the Na^+ hydrogel as an electrolyte for OECTs, we measured output and transfer curves, bandwidth transistor response (transconductance vs frequency), and a cycle test to probe the performance of the OECT under prolonged electrical stress. For comparison, the same tests were carried out on an OECT using the same device architecture and 0.1M NaCl aqueous solution as electrolyte. The OECTs channel dimensions was 100x100 μm^2. Fig. 3b and S5 present the output and transfer curves for both the Na^+ hydrogel and 0.1M NaCl liquid electrolyte, showing similar output characteristics with a peak transconductance of ~3.5 mS. In the case of the liquid electrolyte we observed a shift at slightly higher gate potential of the maximum transconductance (V_G=0.1V). However, drain currents were similar in both electrolytes. Fig. 3c shows the dependence of the transistor transconductance with frequency. In this measurement, the device channel was continuously biased with a V_D=−0.5 V while at the gate a sinusoidal bias was applied (ΔVgs = 25 mV) in the frequency range between 1Hz to 20kHz. When using a liquid electrolyte (0.1M NaCl), we measured at low frequency transconductance values of ~3.6 mS that remain at about this level until 100 Hz. This is followed by an abrupt decrease in the device transconductance, with a cut-off frequency (-3 dB) of 429 Hz. Interestingly, when we performed the same measurement in the presence of the Na^+ hydrogel as the transistor electrolyte we observed almost identical behaviour. A maximum transconductance of ~3.3 mS was measured until 100 Hz as before, followed by a rapid decrease. In this case we had a cut-off frequency of 525 Hz, comparable to the one obtained for the liquid electrolyte. The success of the studied solid electrolyte can be explained by its high ionic conductivity in the same order of magnitude as NaCl 0.1M solution which has a conductivity of 10^{-2} S cm^{-1}.[26] These results clearly showed that the operation the OECT in the presence of the Na^+ hydrogel was unaltered and the Na^+ hydrogel had sufficient ion mobility to perform fast doping/de-doping of the transistor channel.

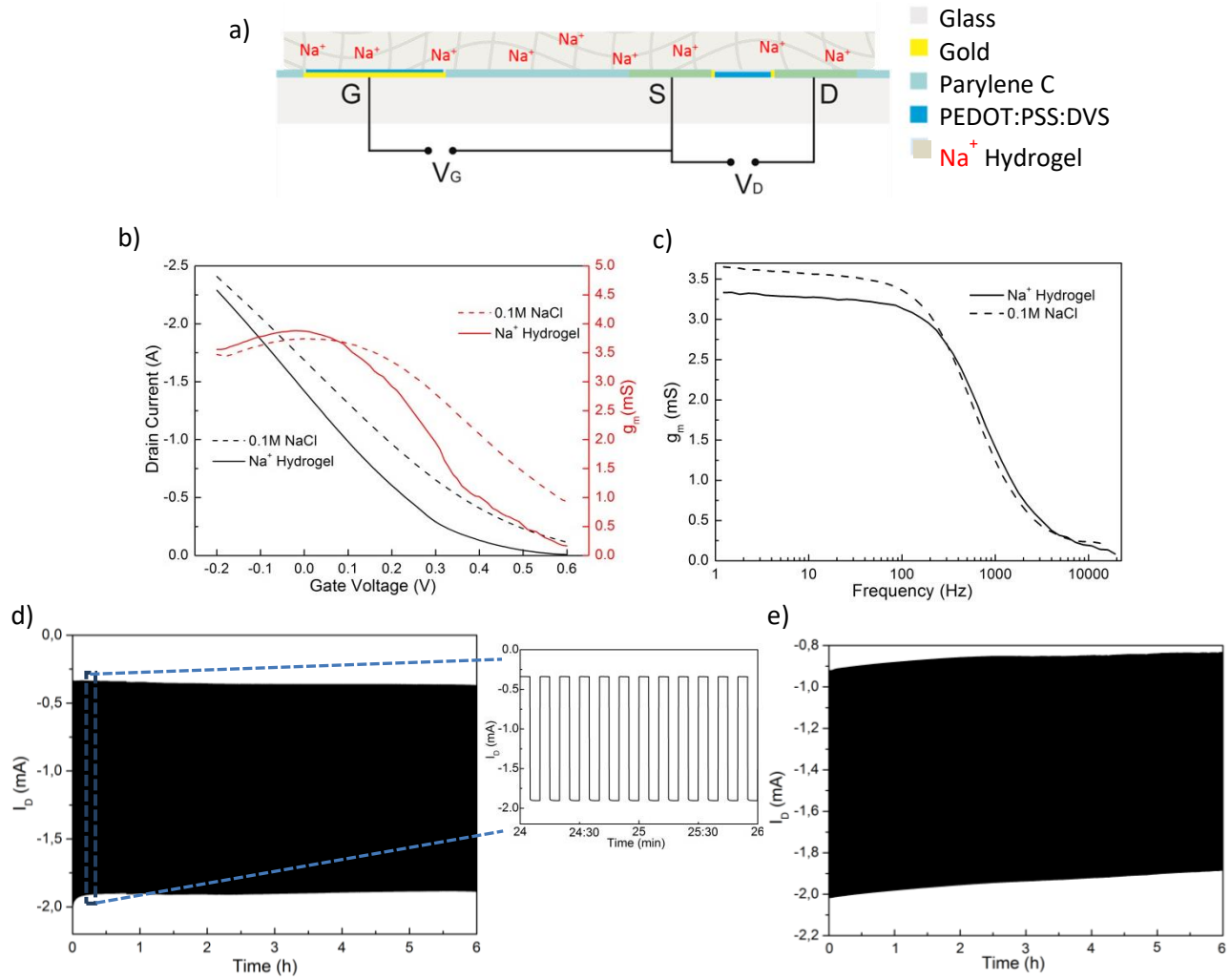

Figure 3 OECT performance and long-term measurements with the hydrogel and NaCl 0.1M solution as the electrolytes. (a) Planar OECT schema and hydrogel on top, (b) hydrogel and 0.1M NaCl IV transfer curve (black) and transconductance (red) in the range of V_G= −0.2V to 0.6 V, (c) hydrogel and 0.1M NaCl bandwidth measurements (transconductance vs frequency), (d) hydrogel cycle test 6 h operation and hydrogel drain current during 2 min of a 6 h operation, and (e) NaCl 0.1M solution cycle test 6 h operation.

In additional to the frequency dependant response and output curves, we were also interested to test the long-term stability of the device in the presence of the Na^+ hydrogel. In order to check the long-term performance of the device, a stress-study of the OECT under high duty conditions was carried out for 6 h.

In this experiment the gate voltage was pulsed from 0 V to 0.5 V every 5 seconds while the drain electrode was kept at -0.5V.

The results of Fig.3d show that the OECT transistor channel pulse response was stable over time. When we started the measurement, we obtained a maximum and minimum current of −1.91 and −0.34 mA, respectively. After 6 hours of the high duty gate pulsing, the final maximum and minimum currents were −1.85 and −0.2 mA, respectively. Overall we observed only a 3.14 % decrement in the maximum current during 6 h of operation. However, the minimum current decreased in the same way, maintaining ΔI_D constant. Inset graph of Fig.3d shows a two minutes pulse time interval where fast device switching from the dope to the de-doped state is observable. Comparable results were obtained to the ones reported above when using 0.1M NaCl solution as the transistor electrolyte.

In conclusion, we showed here that the Na^+ hydrogel can be used as the electrolyte to operate OECTs. The hydrogel presents high ionic conductivity (10^{-2} S cm^{-1}) in the same order of magnitude of the one of NaCl 0.1M aqueous solution (10^{-2} S cm^{-1}).[26] Furthermore, we believe that the high content of water within the structure of the hydrogel (83% w/w) was also responsible of good hydration and swelling of the PEDOT:PSS film, that in turns improves the ionic mobility within the conducting polymer film and provide similar OECT performance when compared to liquid electrolyte.[24,27 28]

Experimental

Na^+ conducting hydrogels synthesis and characterization

A chemically cross-linked Na^+ hydrogel was synthetized by UV-polymerization. For 1 g of hydrogel solution, 0.11 g of poly(ethylene glycol) acrylate (Mw = 375 g mol^{-1}), 0.02 g of poly(ethylene glycol) diacrylate (Mw = 575 g mol^{-1}), 0.04g of sodium acrylate, and 5.1 mg of the photoinitiator 2-hydroxy-4'-

(2-hydroxyethoxy)-2-methylpropiophenone were dissolved in in 0.83 g of DI water (Milli Q). Solution was purged with N_2 and irradiated with UV light during 20 min for polymerization. A UV chamber from Boekel scientific was used for hydrogel crosslinking, model 234100. All reagents come from Sigma-Aldrich. Hydrogels with other water contents (63, 43, and 3 %w/w) were synthetized using the same procedure and maintaining the same monomer ratios. A Bruker ALPHA FTIR spectrometer was used to record IR spectra. The spectra were collected using 32 scans with a resolution of 2 cm⁻1 in the ATR mode. An Environmental Scanning Electron Microscope (ESEM-FEI QUANTA 250) was used to acquire picture of the wet hydrogels at a 100% relative humidity and 2 °C. ^{1}H-NMR spectra have been collected with a Bruker Advance 400 MHz, using D_2O from Deutero GmbH. For Rheological measurements an AR-1500EX instrument was employed from TA instruments equipped with a Peltier system for temperature control. Two types of measurements with a 40mm steel plate were performed. A frequency sweep step experiment (frequency 100-0.1Hz, strain 0.4%, at 25 °C), and a temperature ramp step experiment (temperature 25-75 °C, ramp 3 °C min^{-1}, frequency 1Hz, strain 0.4%). For Electrochemical Impedance Spectroscopy (EIS) measurements, an Autolab PGSTAT302N equipment with a Microcell HC from Metrohm was used. Hydrogel discs with a diameter of 12 mm and thickness of 1.5 mm were placed in between two stainless steel blocking electrodes. EIS was measured at range of temperatures from 10 to 70 °C at a frequency range of 100 kHz to 1 Hz. The ionic conductivity of each sample was calculated from to the real part of the complex impedance (R) using the equation below:

$$\sigma = l/A \quad 1/R$$

OECT fabrication and operation

Microscope glass slides were cleaned in an ultrasonic bath for 15 min in a 2 %v/v soap (micro-90) aqueous solution, rinsed in DI water and followed by sonication for another 15 min in isopropanol:acetone 1:1 v/v. After rinsing the glass substrates with DI water and activating them with O_2 plasma, gold electrodes and interconnects were patterned via a lift-off process by spin-coating S1813 photoresist (Shipley) and exposing it with UV light using a SUSS MJB4 contact aligner and developing it in MF-26 developer. First, an adhesion enhancer layer of chrome (10 nm thick) followed by a second layer of gold (100 nm thick) were thermally evaporated onto the glass substrate followed by lift-off process in acetone. Second, an insulation layer of parylene-C (1.7 µm thick) was deposited using A-174 silane as an adhesion promoter. This was followed by spin coating of a layer of soap (2% v/v soap (micro-90)) to avoid the adhesion of a second sacrificial layer of parylene-C (2 µm) which was deposited on top. Reactive ion etching (RIE) was used to define the OECT channel geometry (100x100 µm²), gate electrode (5x5 mm²) and contact pads of the device. A PEDOT:PSS dispersion containing 1% v/v of the crosslinker divinyl sulfone (DVS),[28] 5% v/v of the solvent ethylene glycol and 0.05 % v/v of the surfactant dodecylbenzenesulphonic acid (all from Sigma-Aldrich) was spin-coated at 1500 rpm to obtain a thickness of ~100 nm. OECT channels and gate geometries were obtained by peeling-off the last layer of parylene-C.

Cycle tests were executed with a Keithley instrument 2602A. Data were collected by pulsing the gate bias from 0 to 0.5 V (t pulse 5 s, high duty cycle) whilst applying a drain bias of -0.5 V. For frequency dependent an IV measurements, a Nationan l Instruments PXIe-1062Q was employed. A source-measurement device NI PXIe-4145 was employed to put the transistor channel bias and gate potential was applied with a NI PXI-6289 device. To execute frequency-dependent measurements, gate and output drain currents were registered using two NI-PXI-4071 digital multimeters (DMM). Bandwidth measurements were conducted by applying a sinusoidal bias at the gate (ΔVgs = 25 mV and 1 Hz < f <20 kHz) whilst maintaining a constant bias at the drain (VDs = −0.5 V). A customized LabVIEW program was employed to control measurement parameters.

Conclusions

In this paper, we presented a PEG-based Na^+ conducting hydrogel as electrolyte for organic electrochemical transistors. The hydrogel was synthesized using fast photopolymerization of commercially available monomers such as poly(ethylene glycol)-dimethacrylate and sodium acrylate. Our hydrogel showed a high ionic conductivity at room temperature (10^{-2} S cm^{-1}) as measured by electrochemical impedance spectroscopy. The OECT showed stable operation during a 6 hour long, high duty cycle stress test and as fast switching performance as OECTs with liquid electrolyte. As an added advantage, the synthesis of the hydrogel can be included during the photolithography device fabrication. This hydrogel paves the way for the replacement of liquid electrolytes in high performance OECTs bringing about advantages in terms of device integration and protection due to its possibilities to by printed or integrated into flexible devices.

Conflicts of interest

The authors declare no conflicts of interest.

Acknowledgements

This work was supported by EU through the Projects FP7- PEOPLE-2012-ITN 316832-OLIMPIA and FP7-PEOPLE- 2013-ITN 607896-OrgBio. A. S-S. is thankful for the Marie Curie IF BIKE Project No. 742865. The authors would like to thank Dr. Christopher Tollan for environmental SEM pictures.

Notes and references

1 K. Nagamine, S. Chihara, H. Kai, H. Kaji and M. Nishizawa, *Sens. Actuators B Chem.*, 2016, **237**, 49–53.
2 M. Braendlein, T. Lonjaret, P. Leleux, J.-M. Badier and G. G. Malliaras, *Adv. Sci.*, 2016, **4**, 1600247.

3 W. Lee, D. Kim, N. Matsuhisa, M. Nagase, M. Sekino, G. G. Malliaras, T. Yokota and T. Someya, *Proc. Natl. Acad. Sci.*, 2017, 201703886.
4 X. Ji, H. Y. Lau, X. Ren, B. Peng, P. Zhai, S.-P. Feng and P. K. L. Chan, *Adv. Mater. Technol.*, 2016, **1**, 1600042–1600050.
5 I. Gualandi, D. Tonelli, F. Mariani, E. Scavetta, M. Marzocchi and B. Fraboni, *Sci. Rep.*, 2016, **6**, 35419.
6 T. Blaudeck, P. A. Ersman, M. Sandberg, S. Heinz, A. Laiho, J. Liu, I. Engquist, M. Berggren and R. R. Baumann, *Adv. Funct. Mater.*, 2012, **22**, 2939–2948.
7 P. Gkoupidenis, D. A. Koutsouras and G. G. Malliaras, *Nat. Commun.*, 2017, **8**, 15448.
8 A. Giovannitti, D.-T. Sbircea, S. Inal, C. B. Nielsen, E. Bandiello, D. A. Hanifi, M. Sessolo, G. G. Malliaras, I. McCulloch and J. Rivnay, *Proc. Natl. Acad. Sci.*, 2016, **113**, 12017–12022.
9 A. Giovannitti, C. B. Nielsen, D.-T. Sbircea, S. Inal, M. Donahue, M. R. Niazi, D. A. Hanifi, A. Amassian, G. G. Malliaras, J. Rivnay and I. McCulloch, *Nat. Commun.*, 2016, **7**, 13066.
10 L. Contat-Rodrigo, C. Pérez-Fuster, J. Lidón-Roger, A. Bonfiglio and E. García-Breijo, *Sensors*, 2016, **16**, 1599.
11 J. Rivnay, P. Leleux, M. Ferro, M. Sessolo, A. Williamson, D. A. Koutsouras, D. Khodagholy, M. Ramuz, X. Strakosas, R. M. Owens, C. Benar, J.-M. Badier, C. Bernard and G. G. Malliaras, *Sci. Adv.*, 2015, **1**, e1400251–e1400251.
12 D. Khodagholy, J. Rivnay, M. Sessolo, M. Gurfinkel, P. Leleux, L. H. Jimison, E. Stavrinidou, T. Herve, S. Sanaur, R. M. Owens and G. G. Malliaras, *Nat. Commun.*, 2013, **4**, 2133.
13 J. Rivnay, R. M. Owens and G. G. Malliaras, *Chem. Mater.*, 2014, **26**, 679–685.
14 Z. Yi, G. Natale, P. Kumar, E. D. Mauro, M.-C. Heuzey, F. Soavi, I. I. Perepichka, S. K. Varshney, C. Santato and F. Cicoira, *J. Mater. Chem. C*, 2015, **3**, 6549–6553.
15 M. Irimia-Vladu, E. D. Glowacki, N. S. Sariciftci and S. Bauer, *Green Materials for Electronics*, John Wiley & Sons, 2017.
16 I. Noshadi, B. W. Walker, R. Portillo-Lara, E. Shirzaei Sani, N. Gomes, M. R. Aziziyan and N. Annabi, *Sci. Rep.*, 2017, **7**, 4345.
17 E. M. Ahmed, *J. Adv. Res.*, 2015, **6**, 105–121.
18 E. Caló and V. V. Khutoryanskiy, *Eur. Polym. J.*, 2015, **65**, 252–267.
19 S. H. Kim, K. Hong, W. Xie, K. H. Lee, S. Zhang, T. P. Lodge and C. D. Frisbie, *Adv. Mater.*, 2013, **25**, 1822–1846.
20 Q. Thiburce, L. Porcarelli, D. Mecerreyes and A. J. Campbell, *Appl. Phys. Lett.*, 2017, **110**, 233302.
21 J. W. Hwang, S. M. Noh, B. Kim and H. W. Jung, *J. Appl. Polym. Sci.*, **132**, 441939–441945.
22 M. Hahn, L. Taite, J. Moon, M. Rowland, K. Ruffino and J. West, *Biomaterials*, 2006, **27**, 2519–2524.
23 Y. S. Kim, K. Cho, H. J. Lee, S. Chang, H. Lee, J. H. Kim and W.-G. Koh, *React. Funct. Polym.*, 2016, **109**, 15–22.
24 E. Stavrinidou, P. Leleux, H. Rajaona, D. Khodagholy, J. Rivnay, M. Lindau, S. Sanaur and G. G. Malliaras, *Adv. Mater.*, 2013, **25**, 4488–4493.
25 C. Karunakaran, K. Bhargava and R. Benjamin, *Biosensors and Bioelectronics*, Elsevier, 2015.
26 G. Xie, F. He, X. Liu, L. Si and D. Guo, *Sci. Rep.*, 2016, **6**, 25002.
27 T. Darmanin and F. Guittard, *Mater. Chem. Phys.*, 2014, **146**, 6–11.
28 D. Mantione, I. del Agua, W. Schaafsma, M. ElMahmoudy, I. Uguz, A. Sanchez-Sanchez, H. Sardon, B. Castro, G. G. Malliaras and D. Mecerreyes, *ACS Appl. Mater. Interfaces*, 2017, **9**, 18254–18262.

TOC